

Optoelectronic Oscillator for Photonic Systems

X. Steve Yao and Lute Maleki, *Member, IEEE*

Abstract—We describe a novel photonic oscillator that converts continuous-light energy into stable and spectrally pure microwave signals. This optoelectronic oscillator (OEO) consists of a pump laser and a feedback circuit including an intensity modulator, an optical-fiber delay line, a photodetector, an amplifier, and a filter. We present the results of a quasi-linear theory for describing the properties of the oscillator and their experimental verifications. Our findings indicate that the OEO can generate ultrastable, spectrally pure microwave-reference signals up to 75 GHz with a phase noise lower than -140 dBc/Hz at 10 KHz. We show that the OEO is a special voltage-controlled oscillator with an optical-output port and can be synchronized to a reference source by means of optical injection locking, electrical injection locking, and a phase-locked loop. Other OEO applications include high-frequency reference regeneration and distribution, high-gain frequency multiplication, comb frequency and pulse generation, carrier recovery, and clock recovery.

I. INTRODUCTION

PHOTONIC radio-frequency (RF) systems [1]–[3] embed photonic technology into the traditional RF systems. In particular, in a photonic RF system, optical waves are used as a carrier to transport RF signals through optical fibers to remote locations. In addition, some of the RF signal-processing functions such as signal mixing [4], antenna-beam steering [5], [6], and signal filtering [7], [8] can also be accomplished optically. The photonic technology offers the advantages of low loss, light weight, high frequency, high security, remoting capability, and immunity to electromagnetic interference.

Traditional RF oscillators cannot meet all the requirements of photonic RF systems. Because photonic RF systems involve RF signals in both optical and electrical domains, an ideal oscillator for the photonic systems should be able to generate RF signals in both optical and electrical domains. In addition, it should be possible to synchronize or control the oscillator by both electrical and optical references or signals.

Presently, generating a high-frequency RF signal in the optical domain is usually done by modulating a diode laser or an external electrooptical (E/O) modulator using a high-frequency stable electrical signal from a local oscillator (LO). Such a local-oscillator signal is generally obtained by multiplying a low-frequency reference, (e.g., quartz oscillator) to the required high frequency, say 32 GHz, with several stages of multipliers and amplifiers. Consequently, the resulting system is bulky, complicated, inefficient, high phase noise, and costly. An alternative way to generate photonic RF carriers is to mix two lasers with different optical frequencies [9]. However,

the resulting bandwidth of the signal is wide (limited by the spectral width of the lasers, typically greater than tens of kilohertz), and the frequency stability of the beat signal is poor, caused by the drift of the optical frequency of the two lasers.

We report here a novel photonic oscillator [10]–[12] that meets the special requirements for the photonic RF systems and yet is extremely suitable for conventional RF applications as well. As will be shown in Fig. 1, this oscillator is based on converting the continuous-light energy from a pump laser to RF and microwave signals, and thus we refer to it with the acronym OEO for optoelectronic oscillator. This oscillator is capable of generating stable signals at frequencies up to 75 GHz (limited by the speed of E/O modulator [13]) in both electrical and optical domains. We present the results of a quasi-linear theory for the threshold condition, the amplitude, the frequency, the linewidth, and the spectral power density of the oscillation. We also present experimental data to compare with the theoretical results. We show that the OEO is a special voltage-controlled oscillator (VCO) with both optical and electrical outputs. It can be used to make phase-locked loop (PLL) and perform all functions that a PLL is capable of for photonic systems. It can also be phase-locked to a remote reference through optical injection and thus is useful for high-frequency reference regeneration and distribution. We will also demonstrate carrier recovery, clock recovery, high-gain frequency multiplication, and comb frequency and pulse generation using the OEO. By using self-phase-locked loop and self-injection locking techniques, high-stability photonic mm-wave references can be generated with the OEO.

The ring configuration consisting of an electrooptic modulator which is fed back with a signal from the detected light at its output has been previously studied by a number of investigators interested in the nonlinear dynamics of bistable optical devices [14]–[18]. The use of this configuration as a possible oscillator was first suggested by Neyer and Voges [19]. However, the interest of their investigations was primarily focused on the nonlinear regime and the chaotic dynamics of the oscillator. Our studies, by contrast, are specifically focused on the stable oscillation dynamics, the noise properties of the oscillator, and its applications in photonic communication systems.

II. DEVICE DESCRIPTION

In an OEO [10]–[12], light from one of the output ports of the E/O modulator is detected by the photodetector and then is amplified, filtered, and fed back to the electrical-input port of the modulator, as shown in Fig. 1(a). If the modulator is properly biased and the small-signal gain of the feedback loop is properly chosen, self-electrooptic oscillation will be

Manuscript received November 2, 1995. This work was supported in part by the Jet Propulsion Laboratory under a contract with the National Aeronautics and Space Administration.

The authors are with the Jet Propulsion Laboratory, California Institute of Technology, Pasadena, CA 91109 USA.

Publisher Item Identifier S 0018-9197(96)05030-0.

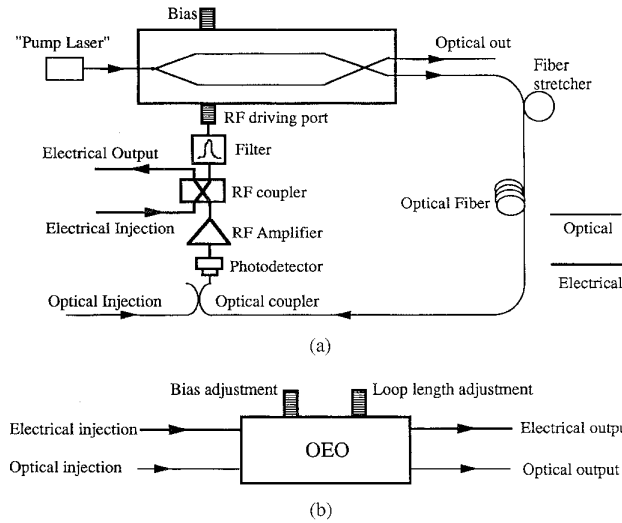


Fig. 1. Device description of the OEO. (a) Device construction. (b) Functional diagram.

sustained. Because both optical and electrical processes are involved in the oscillation, both the optical subcarrier and the electrical signal will be generated simultaneously. Note that this ring oscillator is inherently unidirectional and immune to the back reflections in the loop.

The OEO can be represented by a simple functional block diagram, shown in Fig. 1(b). It is a six-port device, with both optical- and electrical-injection ports, both optical- and electrical-output ports, and two voltage-controlling ports. One of the controlling ports is simply the bias port of the E/O modulator, and the other one is connected to a fiber stretcher for controlling the loop length. As will be shown below, the two injections ports can be used to injection-lock the OEO to a reference source either optically or electrically. The two output ports provide outputs with an RF carrier in both optical and electrical forms. Finally, the two controlling ports can be used to tune the oscillation frequency and to make the OEO a VCO. The six ports collectively make interfacing the oscillator and a photonic RF system very simple.

We have built several such OEO's using different modulators and generated optical subcarriers as high as 9.2 GHz, using a diode-pumped YAG laser at 1310 nm. Fig. 2(a) shows the generated RF signal at 9.2 GHz, and Fig. 2(b) shows the generated signal at 100 MHz. In both cases, the OEO's were free-running, and no effort was made to reduce the noise. For comparison, signal from a HP8656A signal generator is also shown in Fig. 2(b), and the OEO clearly has higher spectral purity than the HP8656A.

III. FUNDAMENTAL CHARACTERISTICS OF THE OEO

A. Threshold Condition

The threshold condition for the OEO can be derived by setting the small-signal gain of the feedback loop, consisting of the E/O modulator, the photodetector, and the RF amplifier, to unity. The signal $V_{out}(t)$ at the output port of the amplifier corresponding to an input signal $V_{in}(t)$ at the driving port of

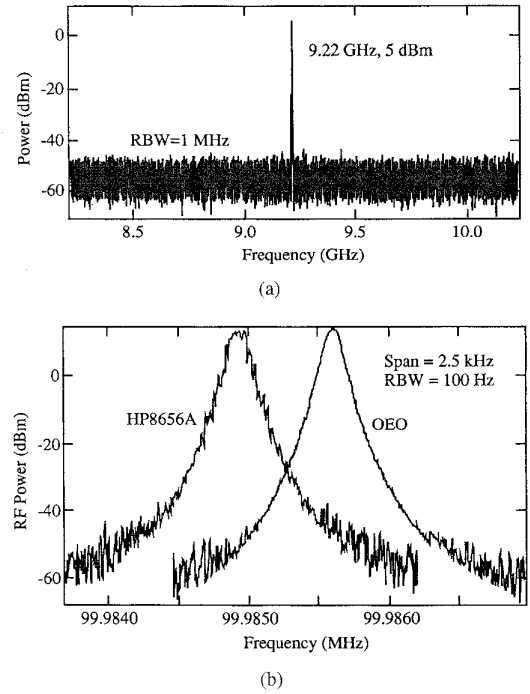


Fig. 2. Spectra of free-running OEO's. (a) Oscillation at 9.22 GHz. (b) Oscillation at 100 MHz.

the E/O modulator can be expressed as

$$V_{out}(t) = V_{ph} \{1 - \eta \sin \pi [V_{in}(t)/V_{\pi} + V_B/V_{\pi}]\} \quad (1)$$

where $V_{ph} \equiv I_{ph} R G_A$ is the photon-generated voltage at the output of the amplifier, R is the load impedance of the detector, G_A is the amplifier's voltage gain, $I_{ph} \equiv \alpha P_0 \rho / 2$ is the detected photocurrent, P_0 is the input optical power, ρ is the responsivity of the detector, α is the fractional insertion loss of the modulator, V_B is its bias voltage, V_{π} is its half-wave voltage, and η determines the extinction ratio of the modulator by $(1 + \eta)/(1 - \eta)$. From (1), the small-signal gain of the loop can be obtained

$$G_S \equiv \left. \frac{dV_{out}}{dV_{in}} \right|_{V_{in}=0} = -\frac{\eta \pi V_{ph}}{V_{\pi}} \cos \left(\frac{\pi V_B}{V_{\pi}} \right). \quad (2)$$

Setting $|G_S| = 1$ yields the threshold condition for the OEO

$$V_{ph} = V_{\pi} / \pi \quad (3)$$

where $\eta = 1$ and $V_B = 0$ or V_{π} are assumed.

It is important to notice that the amplifier in the loop is not a necessary condition for oscillation. So long as $I_{ph} R \geq V_{\pi} / \pi$ is satisfied, no amplifier is needed ($G_A = 1$). It is the optical power from the pump laser that actually supplies the necessary energy for the OEO. This property is of practical significance because it enables the OEO to be powered remotely using an optical fiber. Perhaps more significantly, however, the elimination of the amplifier in the loop also eliminates the amplifier noise, resulting in a more stable oscillator. For a modulator with a V_{π} of 3.14 V and an impedance R of 50 Ω , a photocurrent of 20 mA is required for sustaining the photonic oscillation without an amplifier. This corresponds to

an optical power of 25 mW, assuming the responsivity ρ of the photodetector to be 0.8 A/W.

B. Oscillation Frequency and Amplitude

Equation (1) is nonlinear but can be linearized if we force the signal to pass through a RF filter with a bandwidth sufficiently narrow to block all harmonic components. The linearization process [12] yields

$$V_{\text{out}}(t) = G(V_o)V_{\text{in}}(t) \quad (4)$$

where V_o is the amplitude of the input signal and $G(V_o)$, the voltage-gain coefficient, is defined as

$$G(V_o) = G_S \frac{2V_\pi}{\pi V_o} J_1\left(\frac{\pi V_o}{V_\pi}\right) \quad (5)$$

or approximately as

$$G(V_o) = G_S \left[1 - \frac{1}{2} \left(\frac{\pi V_o}{2V_\pi}\right)^2 + \frac{1}{12} \left(\frac{\pi V_o}{2V_\pi}\right)^4 \right]. \quad (6)$$

For a small-enough input signal ($V_o \ll V_\pi$), we can recover from (5) and (6) the small-signal open-loop gain of $G(V_o) = G_S$.

Although (4) is linear, the linearity coefficient $G(V_o)$ is a nonlinear function of input amplitude and therefore the nonlinear properties of the modulator is not lost. Because of the quasi-linear relation, superposition principle holds so that we can use the regenerative-feedback model [20], [21] to analyze the OEO. From the analysis, we obtain the four most important parameters of the OEO: the frequency f_{osc} , the oscillation amplitude V_{osc} , the linewidth and the oscillation-power spectral density $S_{\text{RF}}(f')$. The obtained oscillation frequency is

$$f_{\text{osc}} = (k + 1/2)/\tau \quad \text{for } G(V_{\text{osc}}) < 0 \quad (7a)$$

$$f_{\text{osc}} = k/\tau \quad \text{for } G(V_{\text{osc}}) > 0 \quad (7b)$$

where k is an integer, representing different possible oscillating modes and τ is the total group delay of the loop, including the physical-length delay of the loop and the group delay resulting from dispersive components in the loop. For all practical purposes, the sign of $G(V_{\text{osc}})$ is determined by the small-signal gain G_S . It is interesting to notice from (7) that the oscillation frequency depends on the biasing polarity of modulator. For negative biasing ($G_S < 0$), the fundamental frequency is $1/(2\tau)$, while for positive biasing ($G_S > 0$), the fundamental frequency is doubled to $1/\tau$.

The oscillation amplitude can be determined by setting $|G(V_{\text{osc}})| = 1$, which yields

$$\left| J_1\left(\frac{\pi V_{\text{osc}}}{V_\pi}\right) \right| = \frac{1}{2|G_S|} \frac{\pi V_{\text{osc}}}{V_\pi} \quad \text{using (5)} \quad (8a)$$

$$V_{\text{osc}} = \frac{2\sqrt{2}V_\pi}{\pi} \sqrt{1 - \frac{1}{|G_S|}} \quad (8b)$$

keeping second-order term in (6)

$$V_{\text{osc}} = \frac{2\sqrt{3}V_\pi}{\pi} \left(1 - \frac{1}{\sqrt{3}} \sqrt{\frac{4}{|G_S|} - 1} \right)^{1/2} \quad (8c)$$

keeping all terms in (6).

Equation (8a) can be solved graphically. Note that this result is the same as that obtained by Neyer and Voges [19] using a more complicated approach. The threshold condition of $|G_S| \geq 1$ is clearly indicated in (8b) and (8c). Fig. 3(a) shows the normalized oscillation amplitude as a function of $|G_S|$ obtained from (8a), (8b), and (8c), respectively. Comparing the three theoretical curves, one can see that for $|G_S| \leq 1.5$, (8b) is a good approximation. For $|G_S| \leq 3$, (8c) is a good approximation.

We measured the oscillation amplitudes of the OEO for different small-signal gains at an oscillation frequency of 100 MHz, and the data obtained is plotted in Fig. 3(b). It is evident that the experimental data agreed well with our theoretical predictions. In the experiment, the output 1-dB compression power of the amplifiers chosen is much larger than the input 1-dB compression power of the modulator, so that the oscillation power is limited by the nonlinearity of the modulator.

C. Spectral Density

Finally, the power-spectral density of the OEO is found [12] to be

$$S_{\text{RF}}(f') = \frac{\delta}{(\delta/2\tau)^2 + (2\pi)^2(\tau f')^2} \quad (9)$$

where f' is the frequency offset from the oscillation frequency f_{osc} and δ is the noise-to-signal ratio of the OEO and is defined as

$$\delta \equiv \rho_N G_A^2 / P_{\text{osc}} \quad (10)$$

where ρ_N is the total noise-density input to the oscillator and is the sum of the thermal noise $\rho_{\text{thermal}} = 4k_B T(NF)$, the shot noise $\rho_{\text{shot}} = 2eI_{\text{ph}}R$, and the laser's relative-intensity noise (RIN) $\rho_{\text{RIN}} = N_{\text{RIN}}I_{\text{ph}}^2R$ densities [16], [17]:

$$\rho_N = 4k_B T(NF) + 2eI_{\text{ph}}R + N_{\text{RIN}}I_{\text{ph}}^2R \quad (11)$$

where k_B is the Boltzman constant, T is the ambient temperature, NF is the noise factor of the RF amplifier, e is the electron charge, I_{ph} is the photocurrent across the load resistor of the photodetector, and N_{RIN} is the RIN noise of the pump laser. In (9) $2\pi f'\tau \ll 1$ is assumed.

It can be seen from (9) that the spectral density of the oscillating mode is a Lorentzian function of frequency. Its full width at half-maximum (FWHM) Δf_{FWHM} is

$$\Delta f_{\text{FWHM}} = \frac{1}{2\pi} \frac{\delta}{\tau^2} = \frac{1}{2\pi} \frac{G_A^2 \rho_N}{\tau^2 P_{\text{osc}}} \quad (12)$$

It is evident from (12) that Δf_{FWHM} is inversely proportional to the square of loop-delay time and linearly proportional to the input noise to signal ratio δ . For a typical δ of 10^{-16} /Hz and a loop delay of 100 ns (20 m), the resulting spectral width is submilli Hertz. The fractional power contained in Δf_{FWHM} is $\Delta f_{\text{FWHM}} S_{\text{RF}}(0) = 64\%$.

From (12), one can also see that for fixed ρ_N and G_A , the spectral width of an OEO is inversely proportional to the oscillation power, similar to the famous Schawlow-Townes formula [22], [23] for describing the spectral width Δf_{laser} of a laser. However, because both P_{osc} and ρ_N are functions of the photocurrent, the statement that the spectral width of an

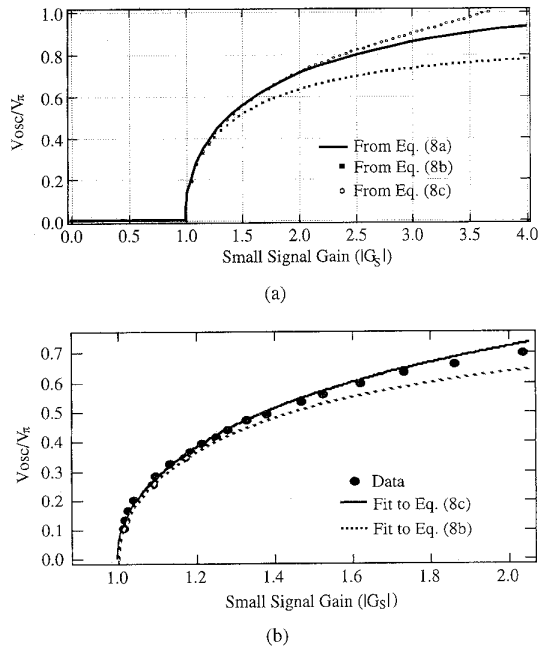


Fig. 3. Normalized oscillation amplitude of an OEO as a function of small-signal gain G_S . (a) Theoretical calculation using (8a), (8b), and (8c). (b) Experimental data and fitting to (8b) and (8c).

OEO is inversely proportional to the oscillation power is only valid when thermal noise dominates in the oscillator at low photocurrent levels.

It can be shown [24] that for an oscillator with a phase fluctuation much less than unity, its power-spectral density is equal to the sum of the single-side band phase-noise density and the single-side-band amplitude-noise density. In most cases in which the amplitude fluctuation is much less than the phase fluctuation, the power-spectral density is just the single-side-band phase noise. Therefore, it is evident from (9) that when $|f'| \gg \Delta f_{FWHM}/2$, the phase noise of the OEO decreases quadratically with the frequency offset f' . For a fixed f' , the phase noise decreases quadratically with the loop-delay time. The larger the τ , the smaller the phase noise. However, the phase noise cannot decrease to zero no matter how large the τ is, because at large enough τ , the assumption $2\pi f'\tau \ll 1$ no longer holds.

Equations (9) and (10) also indicate that the oscillator's phase noise is independent of the oscillation frequency f_{osc} . This result is significant because it allows the generation of high-frequency and low-phase noise signals with the OEO. On the contrary, the phase noise of a signal generated using frequency-multiplying methods generally increases quadratically with the frequency.

We used the frequency-discriminator method [25] to measure the phase noise of the OEO. Fig. 4(a) is the log versus log scale plot of the measured phase noise as a function of the frequency offset f' . Each curve corresponds to a different loop-delay time. Clearly, the phase noise has a 20-dB-per-decade dependence on the frequency offset, in excellent agreement with the theoretical prediction of (9).

Fig. 4(b) is the measured phase noise at 30 kHz from the center frequency as a function of loop-delay time, extracted

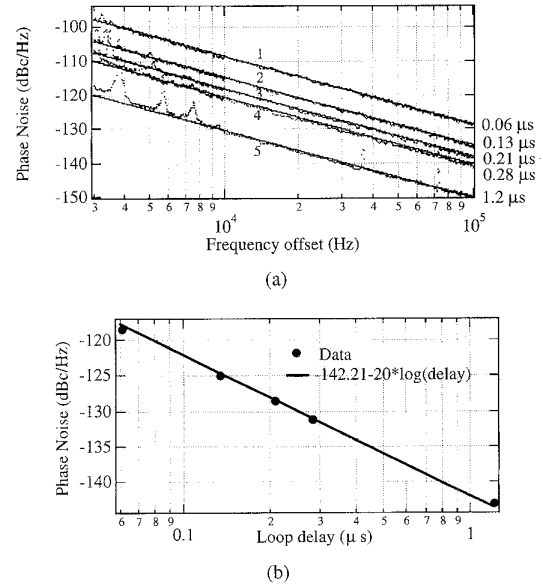


Fig. 4. Single-side-band phase noise of an OEO measured at 800 MHz. (a) Measured phase-noise spectra at different loop delays and their fits to (9). The corresponding loop delays for curves 1–5 are indicated adjacent to each curve, and the corresponding oscillation powers are 16.33, 16, 15.67, 15.67, and 13.33 dBm, respectively. Curve fitting yields the following phase-noise relations as a function of frequency offset f' : $-28.7 - 20 \log(f')$, $-34.84 - 20 \log(f')$, $-38.14 - 20 \log(f')$, $-40.61 - 20 \log(f')$, and $-50.45 - 20 \log(f')$. (b) Phase noise at 30 kHz offset from the center frequency as a function of loop delay. Data points were extracted from curves 1–5 of (a) and were corrected to account for oscillation-power differences.

from the different curves of Fig. 4(a). Because the loop delay is increased by adding more fiber segments, the small-signal gains of the oscillator of longer loops decrease as more segments are connected, causing the corresponding oscillation power to decrease. From the results of Fig. 6 below, the phase noise of the OEO decreases linearly with the oscillation power. To extrapolate the dependence of the phase noise on the loop delay only, each data point in Fig. 4(b) is calibrated using the linear dependence of Fig. 6, while keeping the oscillation power of all data points at 16.33 mW. Again, the experimental data agree well with the theoretical prediction.

To confirm our prediction that the phase noise of the OEO is independent of the oscillation frequency, we measured the phase-noise spectrum as a function of the oscillation frequency, and the result is shown in Fig. 5(a). In the experiment, we kept the loop length at 0.28 μ s and varied the oscillation frequency by changing the RF filter in the loop. The frequency was fine-tuned using an RF stretch-line phase shifter. It is evident from Fig. 5(a) that all of the phase-noise curves at frequencies 100 MHz, 300 MHz, 700 MHz, and 800 MHz overlap with one another, indicating a good agreement with the theory. Fig. 5(b) is a plot of the phase-noise data at 10 kHz as a function of the frequency. As predicted, it is a flat line, in contrast with the case when a frequency multiplier is used to obtain higher frequencies from 100 MHz. This result is significant because it confirms that the OEO can be used to generate high-frequency signals up to 75 GHz with a low phase noise, a performance unattainable with frequency-multiplying techniques.

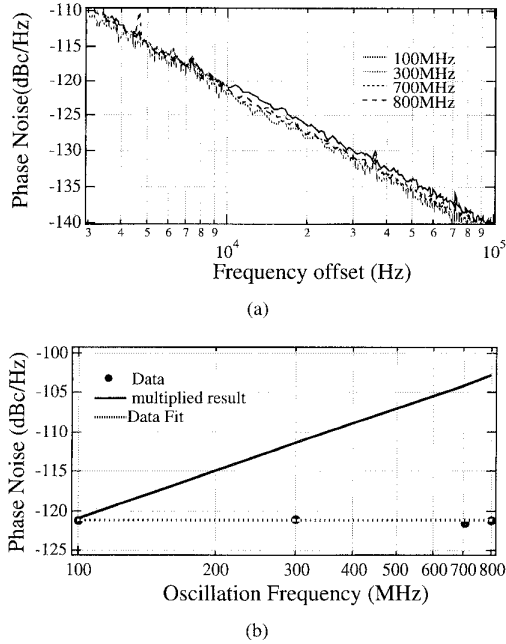


Fig. 5. Single-side-band phase-noise measurements of the OEO at different oscillation frequencies. (a) Phase-noise spectra. (b) Phase noise at 10 kHz offset frequency as a function of oscillation frequency, extracted from (a). The loop delay for the measurements is $0.28 \mu\text{s}$.

We have also measured the phase-noise spectrum of the OEO as a function of oscillation power, and the results are shown in Fig. 6. In that experiment, the loop delay of the OEO was $0.06 \mu\text{s}$, the noise figure of the RF amplifier was 7 dB, and the oscillation power was varied by changing the photocurrent I_{ph} . With this amplifier and the photocurrent level ($\sim 2.5 \text{ mA}$), the thermal noise in the oscillator dominates. Recall that in (9), the phase noise of an OEO is shown to be inversely proportional to the oscillation power. This is true if the gain of the amplifier is kept constant and the photocurrent is low enough to ensure that the thermal noise is the dominant noise term. In Fig. 6(a), each curve is the measurement data of the phase-noise spectrum corresponding to an oscillating power, and the curves in Fig. 6(b) are the fits of the data to (9). Fig. 6(c) is the phase noise of the OEO at 10 kHz as a function of the oscillation power, extracted from the different curves of Fig. 6(b), and agrees well with the theoretical prediction of (9).

IV. VCO FUNCTIONS

As mentioned above, the oscillation frequency of the OEO can be tuned by changing the loop length using a piezoelectric stretcher. The frequency change Δf is given by $\Delta f = -f_o \Delta L / L$, where L is the loop length, ΔL is the loop-length change, and f_o is the nominal oscillation frequency. However, the tuning sensitivity (Hz/volt) is expected to be small.

The oscillation frequency can also be tuned by changing the bias voltage of the E/O modulator. Fig. 7(a) shows that the frequency detuning of the oscillator is linearly proportional to the bias voltage, with a slope of 38.8 kHz/V . The output power of the oscillator remain relatively unchanged in a wide voltage range, as shown in Fig. 7(b). This result is significant because

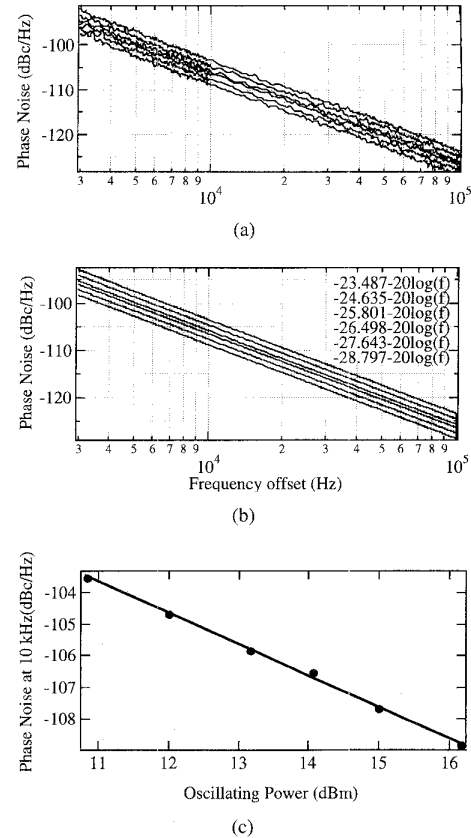


Fig. 6. Single-side-band phase-noise spectra as a function of oscillation power measured at 800 MHz. (a) Experimental data. (b) The fit to (9). (c) Phase noise at 10 kHz offset as a function of oscillation power extracted from (b).

it provided a simple way to tune the oscillation frequency with high sensitivity and is instrumental for realizing PLL using the OEO, as will be discussed next.

V. SYNCHRONIZATION AND STABILIZATION

A. Injection Locking

Injection locking [26], [27] is a commonly used technique for synchronizing an oscillator with a reference frequency. A unique aspect of the OEO is that it can be injection locked by either an optical signal or an electrical signal, as shown in Fig. 1(b). Injection locking an oscillator optically is important because it allows remote synchronization [28], [29]. This function is critical for high-frequency RF systems which require many oscillators locked to a single master, as in a phased-array radar [2], [28]. Another advantage of optical injection locking is that the locking oscillator is electrically isolated from the locked oscillator, eliminating the need for impedance matching between the oscillators.

Fig. 8(a) shows the experimental results of injection locking the OEO with a maser reference at 100 MHz through the electrical-injection port. Similar results are expected for optical injection since the optical-injection signal will first be converted to an electrical signal by an internal photodetector in the loop before affecting the E/O modulator. As shown in

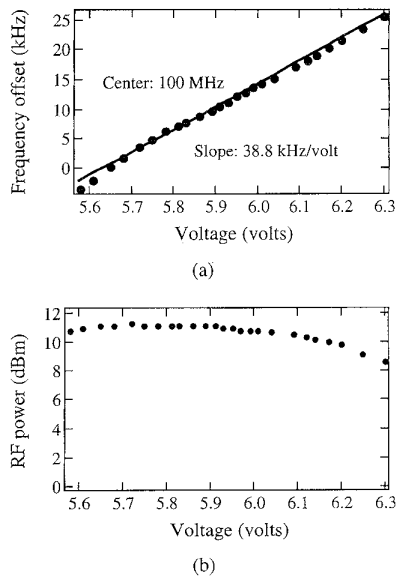


Fig. 7. Demonstration of the capability of tuning the OEO's frequency by controlling the bias voltage of the E/O modulator. (a) Frequency versus bias voltage. (b) Oscillation power versus bias voltage.

Fig. 8(a), with an injection power of -5 dBm, the phase noise of the OEO is almost identical to that of the injecting-maser signal. Note that the output RF power of the OEO is 13 dBm, resulting in a gain of 18 dB. As the injection power decreased, the phase noise of the OEO increased somewhat. However, the output RF power remains the same and therefore the gain is effectively increased. In the experiments, we were able to injection lock the OEO to a maser reference with an injection power as low as -50 dBm.

Fig. 8(b) shows the experimental result of the locking range as a function of injection power. As expected, the locking range is linearly proportional to the square-root of the injection power, agreeing well with Adler's injection-locking theory [26].

B. Self-Injection Locking

Although injection locking is an effective way for synchronizing and stabilizing oscillators, it requires a low-noise and high-stability source to begin with. Making a high-frequency and high-stability source itself is a difficult task. By using a novel scheme called self-injection locking to stabilize the OEO, the OEO may be made as the frequency reference, as illustrated in Fig. 9(a). In this scheme, we derive a small portion of the output optical signal from the OEO and send it through a long fiber-delay line. The output from the fiber-delay line is then converted to electric signal and is fed back to the RF driving port of the E/O modulator. Note that the open-loop gain of this feedback loop should be kept much below unity so that no self-oscillation can be started. Basically, what we do here is to inject a delayed replica of the OEO's output back to the oscillator and force the oscillator to lock to its "past." This will prevent the oscillator from changing its frequency and phase and hence reduce the frequency and phase fluctuations. The frequency stability of the oscillator then is expected to be proportional to the length fluctuation $\Delta L/L$ of the fiber delay

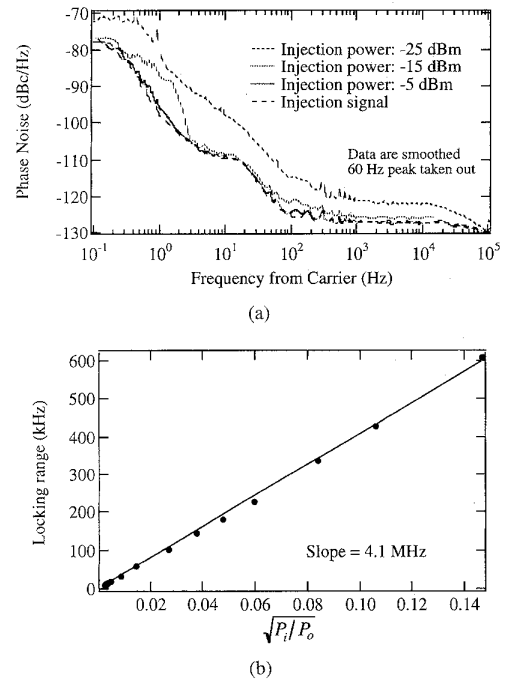


Fig. 8. Demonstration of injection locking the OEO. (a) Phase-noise measurement of the injection-locked oscillator. (b) Locking range as a function of the square-root of the injection power.

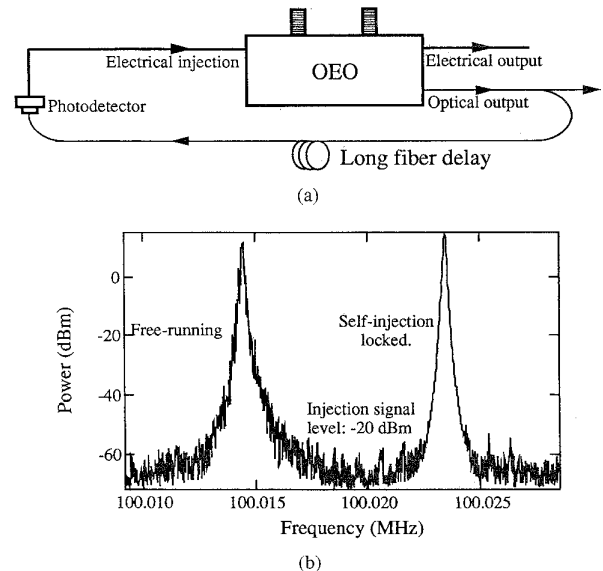


Fig. 9. Demonstration of self-injection locking. (a) Illustration of the self-injection locking concept. (b) Experimental result.

line, which may be stabilized by temperature control against thermal variations.

Fig. 9(b) is the experimental results showing the effectiveness of the self-injection technique in reducing the frequency noise of the OEO. The length of the delay line used in the experiment is 12 km and the feedback injection RF power is -19.23 dBm. It is evident that self-injection locking greatly reduced the frequency fluctuations of the OEO. Further noise reduction is expected if we reduce the length fluctuation of the fiber-delay line by placing it in a temperature-controlled

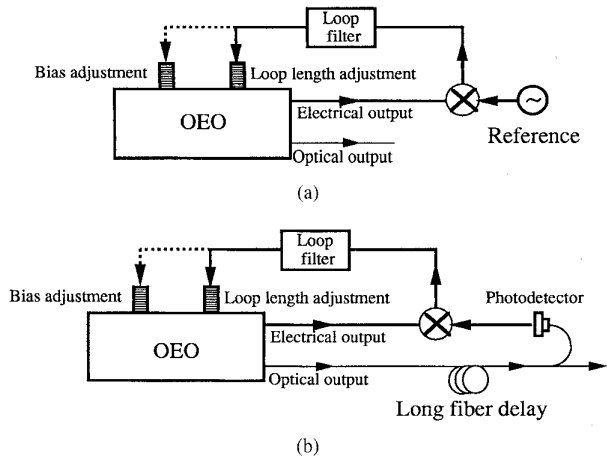


Fig. 10. Illustrations of phase-locking the OEO using a PLL. (a) Phase locking to a reference source. (b) Phase locking to its past or self-phase locking.

environment and isolating it from acoustic vibrations. More experiments are under way to further reduce the noise of the self-injection-locked OEO.

C. PLL

Because the OEO is also a VCO, it can be synchronized to a reference source via a PLL [30], as shown in Fig. 10(a). We have demonstrated this phase-locked loop capability in our laboratory.

D. Self-Phase Locking

As mentioned before, a unique property of the OEO is that it has an optical output. With this optical output, we can make a self-phase-locked loop to stabilize it, as shown in Fig. 10(b). Similar to the self-injection locking described earlier, the self-phase-locked loop forces the oscillator to be locked to its past and reduces its fluctuations.

The technique of delay-line discriminator for stabilizing an oscillator is well known. To effectively stabilize an oscillator, a delay of many kilometers is needed and was therefore considered impractical before the emergence of the photonic technology. In our laboratory we have previously demonstrated [31] the use of a fiber-optic delay line to stabilize a traditional VCO and obtained excellent results. However, in that setup, the fiber-optic delay line included a laser transmitter to convert the VCO's electrical output into optical signal and then transmit the optical signal through a few kilometers of fiber. Since the OEO automatically contains an optical output, it is ideal for using the fiber-delay line technique to stabilize itself without the need of electrical-to-optical signal conversion. Consequently, the device is simple, low-loss, and less expensive.

VI. APPLICATIONS

A. VCO

As mentioned earlier, the OEO is a special VCO with optical as well as electrical output. Therefore it can perform all

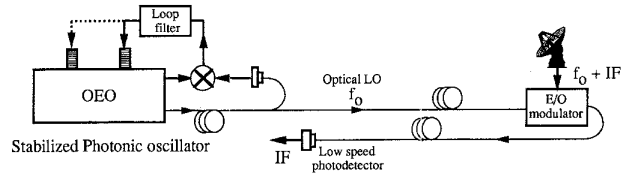


Fig. 11. Illustration of using the OEO for photonic down conversion.

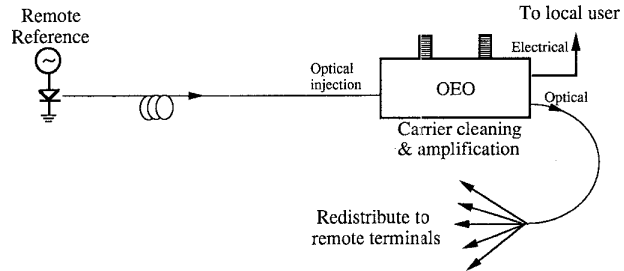


Fig. 12. Illustration of using the OEO for reference regeneration and distribution.

functions that a VCO is capable of for photonic RF systems. These functions include [30] generating, tracking, cleaning, amplifying, and distributing RF carriers. The photonic VCO's in a PLL configuration can also be used for clock recovery, carrier recovery, signal modulation and demodulation, and frequency synthesis.

B. Photonic-Signal Mixing

The OEO can also be used for photonic-signal up/down conversion [4], as shown in Fig. 11. For such an application, a stable optical RF LO, or a modulated optical signal at a RF frequency, is required. The OEO can accomplish just that, since one of its outputs gives the RF oscillation in optical domain.

C. Carrier Distribution

Because the OEO can be injection locked by a remote-optical signal, it can be used for high-frequency RF carrier regeneration, amplification, and distribution, as shown in Fig. 12. Such a capability is important in large photonic RF systems.

D. Frequency Multiplication

The injection-locking property of the OEO can also be used for high-gain frequency multiplication. In the first scheme, as shown in Fig. 13(a), the nonlinearity of the modulator is used and the OEO is injection-locked to an external signal which is a subharmonic of the oscillator's operating frequency. This is the so-called subharmonic injection locking [32]. We have demonstrated phase-locking the oscillator operating at 300 MHz to a 100-MHz reference of 4 dBm. The output of the oscillator is 15 dBm, resulting in a gain of 11 dB and frequency-multiplication factor of 3.

In the second scheme, the nonlinearity of a laser diode [28] is used, as shown in Fig. 13(b). If the laser is biased properly and is driven hard enough, its output will contain

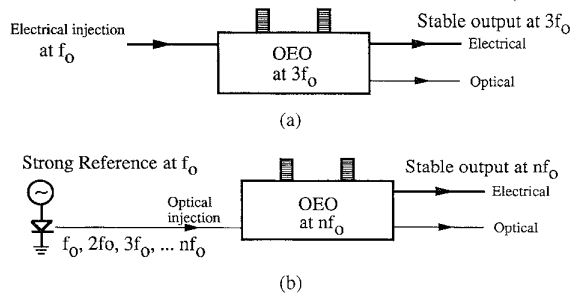


Fig. 13. Illustration of using the OEO for frequency multiplication. (a) Frequency multiplication using OEO's nonlinearity. (b) Frequency multiplication using laser diode's nonlinearity.

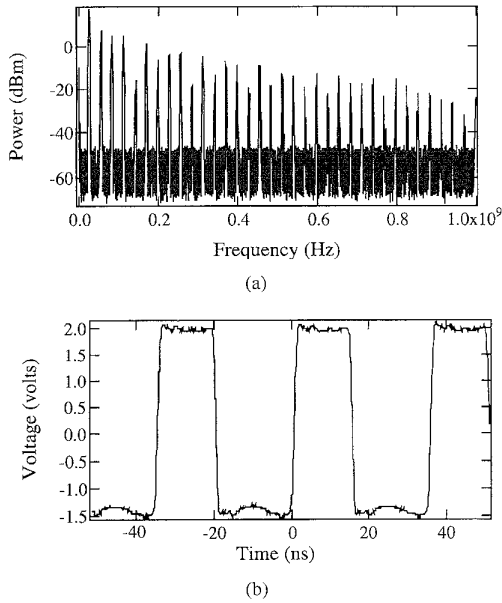


Fig. 14. Demonstration of comb frequency and pulse generation using the OEO. (a) Comb-frequency generation. (b) Square-pulse generation.

many harmonics of the driving signal. The OEO is tuned to operate at a nominal frequency close to the n th harmonic of the reference signal driving the laser diode. Upon the injection of the laser's output, the OEO will be locked to the n th harmonic. This scheme offers remote frequency-multiplication capability [33] and may be useful for many photonic RF system.

E. Comb Frequency and Pulse Generation

The OEO can also be used to generate frequency combs and pulses, as shown in Fig. 14. For this application, the OEO is chosen to operate with multimodes. A sinusoidal signal with a frequency equal to the mode spacing or a multiple of mode spacing is injected into the oscillator. Just like laser mode-locking, this injected signal will force all modes to oscillate in phase. Consequently, we obtain a comb of frequencies that are in phase. In the time domain, the output signal is square pulses.

F. Clock and Carrier Recovery

In high-speed fiber-optic communication systems, the ability of recovering clock from the incoming random data is essential

[34], [35]. The same injection-locking property of the OEO can also be used for clock and carrier recovery. The incoming data is injected into the OEO either optically or electrically. The free-running OEO is tuned to oscillate at a nominal frequency equal to the clock frequency of the incoming data. With the injection of the data, the OEO will be quickly locked to the clock frequency of the data stream while rejecting other frequency components (harmonics and subharmonics) associated with the data. Consequently, the output of the locked OEO is a continuous periodic wave synchronized with the incoming data, or simply the recovered clock. As can be seen, the device has both electrical and optical inputs and both electrical and optical outputs.

We have demonstrated [36], [37] clock recovery at 100 Mb/s and 5 Gb/s and obtained excellent results. Data rates up to 75 Gb/s can also be recovered using the injection-locking technique with a OEO operating at 75 GHz. Note that the data rates at one-half of this value are impossible to achieve with the current electronic clock-recovery techniques. Another important feature of the OEO technique is that the clock can be recovered directly from data just out of a fiber-optic transmission line, without the need of optical-to-electrical conversion. In addition, the recovered clock signal has both optical and electrical forms and is easy to interface with a fiber-optic communication system.

Similar to clock recovery, a carrier buried in noise can also be recovered by the OEO. To do so, we simply inject the spoiled carrier into a OEO that has a free-running frequency close to the carrier and an output power level $N(N \gg 1)$ dB higher than the carrier. The injected carrier forces the OEO to be locked with the carrier and results in an equivalent carrier gain of N dB. Because the small-signal gain of the OEO is only n dB ($n \sim 1$), the noise of the input is only amplified by n dB and the signal-to-noise ratio of the carrier is then increased by $(N - n)$ dB. We have also demonstrated [36], [37] the recovery of carrier from noise and increased carrier-to-noise ratio by 50 dB.

VII. SUMMARY

In summary, we have reported a novel photonic oscillator which we termed OEO. We have presented the theoretical expressions for the oscillation threshold, amplitude, frequency, linewidth, and spectral density of the OEO. These results agree with our experimental data. We have also shown that this device is capable of generating stable signals at frequencies up to 75 GHz and is a special VCO with both optical and electrical output. It can be used to make a PLL and perform all functions that a PLL is capable of for photonic systems. It can be synchronized to a reference source by means of optical-injection locking, electrical-injection locking, and PLL. It can also be self-phase locked and self-injection locked to generate high-stability photonic RF reference. Its applications includes high-frequency reference regeneration and distribution, high-gain frequency multiplication, comb-frequency and square-wave generation, carrier recovery, and clock recovery. We anticipate that such photonic VCO's will be as important to photonic RF systems as electrical VCO's to electrical RF systems.

ACKNOWLEDGMENT

The authors would like to thank G. Lutes and M. Calhoun for many technical discussions and assistance.

REFERENCES

- [1] H. Ogawa, D. Polifko, and S. Banba, "Millimeter-wave fiber optics systems for personal radio communication," *IEEE Trans. Microwave Theory Tech.*, vol. 40, pp. 2285–2293, 1992.
- [2] P. Herczfeld and A. Daryoush, "Fiber optic feed network for large aperture phased array antennas," *Microwave J.*, pp. 160–166, Aug. 1987.
- [3] X. S. Yao and L. Maleki, "Field demonstration of X-band photonic antenna remoting in the deep space network," TDA Progress Rep. 42-117, Jet Propulsion Lab., pp. 29–34, 1994.
- [4] G. K. Gopalakrishnan, W. K. Burns, and C. H. Bulmer, "Microwave-optical mixing in LiNbO₃ modulators," *IEEE Trans. Microwave Theory Tech.*, vol. 41, pp. 2383–2391, 1993.
- [5] E. Toughlian and H. Zmuda, "A photonic variable RF delay line for phased array antennas," *J. Lightwave Technol.*, vol. 8, pp. 1824–1828, 1990.
- [6] X. S. Yao and L. Maleki, "A novel 2-D programmable photonic time-delay device for millimeter-wave signal processing applications," *IEEE Photon. Technol. Lett.*, vol. 6, pp. 1463–1465, 1994.
- [7] D. Norton, S. Johns, and R. Soref, "Tunable wideband microwave transversal filter using high dispersive fiber delay lines," in *Proc. 4th Biennial Dept. of Defense Fiber Opt. and Photon. Conf.*, McLean, VA, 1994, pp. 297–301.
- [8] B. Moslehi, K. Chau, and J. Goodman, "Fiber-optic signal processors with optical gain and reconfigurable weights," in *Proc. 4th Biennial Dept. of Defense Fiber Opt. and Photon. Conf.*, McLean, VA, 1994, pp. 303–309.
- [9] Lightwave Electronics Corp., "Introduction to diode-pumped solid state lasers," Technical information no. 1, 1993.
- [10] X. S. Yao and L. Maleki, "High frequency optical subcarrier generator," *Electron. Lett.*, vol. 30, no. 18, pp. 1525–1526, 1994.
- [11] ———, "Converting light into spectrally pure microwave oscillation," *Opt. Lett.*, vol. 21, no. 7, pp. 483–485, 1996.
- [12] ———, "Opto-electronic oscillator," accepted for publication in *J. Opt. Soc. Amer. B*. Also available in TDA Progress Rep. 42-123, Jet Propulsion Lab., pp. 32–42, 1995.
- [13] K. Noguchi, H. Miyazawa, and O. Mitomi, "75 GHz broadband Ti:LiNbO₃ optical modulator with ridge structure," *Electron. Lett.*, vol. 30, no. 12, pp. 949–951, 1994.
- [14] A. Neyer and E. Voges, "Nonlinear electrooptic oscillator using an integrated interferometer," *Opt. Commun.*, vol. 37, pp. 169–174, 1980.
- [15] ———, "Dynamics of electrooptic bistable devices with delayed feedback," *IEEE J. Quantum Electron.*, vol. QE-18, pp. 2009–2015, 1982.
- [16] H. F. Schlaak and R. Th. Kersten, "Integrated optical oscillators and their applications to optical communication systems," *Opt. Commun.*, vol. 36, no. 3, pp. 186–188, 1981.
- [17] H. M. Gibbs, F. A. Hopf, D. L. Kaplan, M. W. Derstine, R. L. Shoemaker, "Periodic oscillation and chaos in optical bistability: possible guided wave all optical square-wave oscillators," in *SPIE Proc. Integrat. Opt. Millimeter and Microwave Integrat. Circuits*, vol. 317, pp. 297–304.
- [18] E. Garmire, J. H. Marburger, S. D. Allen, and H. G. Winful, "Transient response of hybrid bistable optical devices," *Appl. Phys. Lett.*, vol. 34, no. 6, pp. 374–376, 1979.
- [19] A. Neyer and E. Voges, "High-frequency electro-optic oscillator using an integrated interferometer," *Appl. Phys. Lett.*, vol. 40, no. 1, pp. 6–8, 1982.
- [20] Siegman, *Lasers*. Mill Valley, CA: Univ. Sci. Books, 1986, ch. 11.
- [21] M. F. Lewis, "Some aspects of saw oscillators," in *Proc. 1973 IEEE Ultrasonics Symp.*, pp. 344–347.
- [22] A. L. Schawlow and C. H. Townes, "Infrared and optical masers," *Phys. Rev.*, vol. 112, no. 6, pp. 1940–1949, 1958.
- [23] R. L. Byer, "Diode laser-pumped solid-state lasers," *Science*, vol. 239, pp. 742–747, 1988.
- [24] L. S. Culter and C. L. Searle, "Some aspects of the theory and measurement of frequency fluctuations in frequency standards," *Proc. IEEE*, vol. 54, no. 2, pp. 136–154, 1966.
- [25] Hewlett-Packard Co., "Phase noise characterization of microwave oscillators—Frequency discriminator method," Product note 11729C-2.
- [26] R. Adler, "A study of locking phenomena in oscillators," *Proc. IRE*, vol. 34, pp. 351–357, 1946.
- [27] K. Kurokawa, "Injection locking of microwave solid-state oscillators," *Proc. IEEE*, vol. 61, pp. 1386–1410, 1973.
- [28] A. Daryoush, "Optical synchronization of millimeter-wave oscillators for distributed architectures," *IEEE Trans. Microwave Theory Tech.*, vol. 38, pp. 467–476, 1990.
- [29] Goldberg, C. Rauscher, J. F. Weller, H. F. Taylor, "Optical injection locking of X-band FET oscillator using coherent mixing of GaAs lasers," *Electron. Lett.*, vol. 19, pp. 20, pp. 848–849 1983.
- [30] D. Wolaver, *Phase-Locked Loop Circuit Design*. Englewood Cliffs, NJ: Prentice-Hall, 1991.
- [31] R. Logan, L. Maleki, and M. Shadaram, "Stabilization of oscillator phase using a fiber optic delay-line," in *Proc. 45th Annu. Symp. Frequency Contr.*, Los Angeles, CA, May 29–31, 1991.
- [32] X. Zhang, X. Zhou, and A. Daryoush, "A theoretical study of the noise behavior of subharmonically injection locked local oscillators," *IEEE Trans. Microwave Theory Tech.*, vol. 40, pp. 895–902, 1992.
- [33] A. Daryoush, P. Herczfeld, Z. Turski, and P. Kahi, "Comparison of indirect optical injection locking techniques of multiple X-band oscillators," *IEEE Trans. Microwave Theory Tech.*, vol. MTT-34, pp. 1363–1369, 1986.
- [34] P. E. Barnsley, H. J. Wickes, G. E. Wickens, and D. M. Spirit, "All-optical clock recovery from 5 Gb/s data using a self-pulsation 1.56 mm laser diode," *IEEE Photon. Technol. Lett.*, vol. 3, pp. 942–945, 1991.
- [35] D. M. Patrick and R. J. Manning, "20 Gbit/s all-optical clock recovery using semiconductor nonlinearity," *Electron. Lett.*, vol. 30, no. 2, pp. 151–152, 1994.
- [36] X. S. Yao and G. Lutes, "A high speed photonic clock and carrier regenerator," *IEEE Photon. Technol. Lett.*, vol. 8, pp. 688–690, 1996.
- [37] X. S. Yao, G. Lutes, L. Maleki, and S. Cao, "A novel photonic clock and carrier recovery device," *SPIE Proc., Wireless Communications*, vol. 2556, 1995, pp. 118–127.



X. Steve Yao was born in Hongzhou City, China, in 1960. He received the B.S. degree in physics from the Hebei University, China, in 1982, the M.S. degree in applied physics from the Northwest Telecommunications Engineering Institute, China, in 1984, and the M.S. and Ph.D. degrees in electrical engineering/electrophysics from the University of Southern California, Los Angeles, in 1989 and 1992, respectively.

He joined Jet Propulsion Laboratory, California Institute of Technology, Pasadena, as a Member of Technical Staff in 1990, engaging in the research and development of advanced ultrastable microwave analog fiber-optics devices and systems. He has broad interests in microwave photonics and nonlinear optics and has authored numerous papers in the areas of optically controlled phased array antenna, photonic microwave generation, optical nonlinear effects on fiber communication systems, and optical pulse coupling in photorefractive crystals.

Dr. Yao is a member of the Optical Society of America.



Lute Maleki (M'89) received the B.S. degree in 1969 from the University of Alabama, Tuscaloosa, and the M.S. and Ph.D. degrees in 1972 and 1975, respectively, from Louisiana State University, New Orleans (presently the University of New Orleans), all in physics.

He is the Technical Group Supervisor, Time and Frequency Systems Research Group, at the Jet Propulsion Laboratory, California Institute of Technology, Pasadena. He conducts and directs research in various areas related to the generation, distribution, and characterization of ultrastable frequencies, including the development of trapped ion standards, laser spectroscopy of atoms and ions in discharges, cryogenic cavity stabilized oscillators, the study of noise properties of semiconductor lasers, and fiber-optic frequency distribution systems.